Electron Paramagnetic Resonance Spectrum of Pr^{4+} in $BaCeO_3$

Yukio Hinatsu

Department of Chemistry, Japan Atomic Energy Research Institute, Tokai-mura, Ibaraki 319-11, Japan

and

Norman Edelstein

Chemical Sciences Division, Lawrence Berkeley Laboratory, University of California, Berkeley, California, 94720, USA

The electron paramagnetic resonance spectrum of a powder of Pr^{4+} in $BaCeO_3$ was measured at 8.5 K. A very large hyperfine interaction with the ^{141}Pr nucleus was observed. In addition to the allowed hyperfine transitions, forbidden hyperfine transitions were observed. The results were analyzed based on the weak field approximation, i.e., Breit–Rabi formula, and the g value, $|g| = 0.745(1)$ and the hyperfine coupling constant, $|A| = 0.0606(2)$ cm^{-1}, were obtained. From the measured g value, the $\Gamma_7 \rightarrow \Gamma_8$ crystal field transition for $BaPrO_3$ obtained from an earlier inelastic neutron scattering experiment, and setting the spin–orbit coupling constant to its free ion value $\zeta = 865$ cm^{-1}, the energy levels of Pr^{4+} in $BaCeO_3$ were calculated. The measured magnetic susceptibility of $BaPrO_3$ was compared to the values calculated with the above model. © 1994 Academic Press, Inc.

INTRODUCTION

Perovskite-type oxides, ABO_3, where A is a divalent ion (e.g., Sr, Ba) accommodate tetravalent metal ions at the B sites of the crystals. This perovskite has good thermal stability and is one constituent of the important ceramic waste form known as SYNROC (1). Since tetravalent lanthanide and actinide ions can be incorporated into the B sites, this lattice type is useful for studying the magnetic properties of these ions in octahedral symmetry.

Although the trivalent oxidation state of praseodymium is most stable, the tetravalent state is accessible (2) and has a $4f^1$ electronic configuration outside the closed shell. For electronic structure analysis, the f^1 configuration is straightforward as only the crystal field and spin–orbit coupling interactions are important.

In an earlier study (3), the magnetic susceptibility of $BaPrO_3$ was measured, and a small effective magnetic moment (0.68 μ_B) and a large temperature-independent paramagnetism (TIP) ($\chi_{TIP} = 6.8 \times 10^{-4}$ emu/mole) were reported. Subsequently, we have prepared samples in which Pr^{4+} ions were doped in $BaCeO_3$ (which is isomor-

phous with $BaPrO_3$) and have measured the electron paramagnetic resonance (EPR) spectra at low temperatures. Although the EPR spectrum of $Pr^{4+}/ZrSiO_4$ has been reported previously (4), this work represents the first observation of the EPR spectrum of Pr^{4+} in an octahedral site. The EPR results, together with the earlier magnetic susceptibility measurements, and recent inelastic neutron scattering results on $BaPrO_3$ (5) will be discussed in this paper.

EXPERIMENTAL

Sample Preparation

$BaCO_3$, Pr_6O_{11}, and CeO_2 were used as the starting materials. Before use, the Pr_6O_{11} was reduced to the stoichiometric Pr_2O_3 by heating in a flow of hydrogen gas at 1000°C for 8 hr. CeO_2 was heated in air at 850°C to remove any moisture and to oxidize the material to the stoichiometric composition. The $BaCO_3$, Pr_2O_3, and CeO_2 were weighed in the correct metal ratios ($y = 0.02, 0.05$, and 0.10 for $BaPr_yCe_{1-y}O_3$), intimately mixed, and heated in a flowing oxygen atmosphere at 1300°C in a SiC resistance furnace for a day. After cooling to room temperature, the samples were crushed into powder, reground, repressed into pellets, and then reheated under the same conditions to complete the reaction.

Analysis

An X-ray powder diffraction analysis was obtained with $CuK\alpha$ radiation on a Philips PW 1390 diffractometer equipped with a curved graphite monochromator.

Electron Paramagnetic Resonance Measurement

EPR spectra at X band (9.056 GHz) were measured using a JEOL RE-2X spectrometer operating with an Air Products Helitran cooling system. The magnetic field was

swept from 100 to 13,000 G. Before the samples were measured, a blank was recorded to eliminate the possibility of interference by the background resonance of the cavity and/or the sample tube. The magnetic field was monitored with a proton NMR gaussmeter, and the microwave frequency was measured with a frequency counter. The spectrum covered a magnetic field range of approximately 1 T and the linewidths varied from approximately 20 to 200 G. Thus the accuracy in the measurement of the lines varies and is estimated to be from approximately 5–25 G depending on the particular transition.

RESULTS AND DISCUSSION

For the praseodymium ion in the tetravalent state, an EPR spectrum should be observed because the Pr^{4+} ion is a Kramers ion ([Xe]$4f^1$ configuration). However, no EPR spectra were observed even at 4.2 K for pure $BaPrO_3$, which probably is due to strong magnetic dipole–dipole interactions (3). For three samples of Pr^{4+} doped in $BaCeO_3$ (the praseodymium concentration y is 0.02, 0.05, or 0.10 for $BaPr_yCe_{1-y}O_3$), no EPR spectra were observed at room temperature. At low temperatures, EPR spectra could be observed for two samples, $BaPr_{0.02}Ce_{0.98}O_3$ and $BaPr_{0.05}Ce_{0.95}O_3$. The spectra for $BaPr_{0.05}Ce_{0.95}O_3$ were much weaker in intensity than the spectra for $BaPr_{0.02}Ce_{0.98}O_3$. Figure 1 shows the spectrum for $BaPr_{0.02}Ce_{0.98}O_3$ measured at 8.5 K. This observation of an EPR spectrum strongly indicates that the oxidation state of the praseodymium ion is not trivalent, but tetravalent, because the non-Kramers Pr^{3+} ion usually shows no EPR spectrum (6). The observed spectra are complicated and composed of many absorption lines as shown in Fig. 1.

The isotope ^{141}Pr (natural abundance 100%) has a nuclear spin of $I = \frac{5}{2}$ and a nuclear magnetic moment of
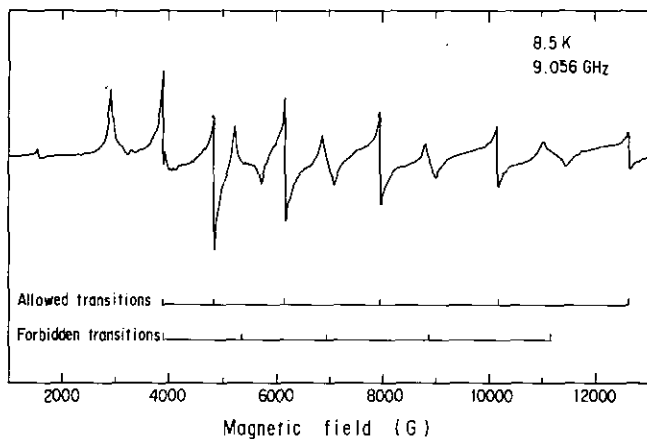
FIG. 1. EPR spectrum of $BaPr_{0.02}Ce_{0.98}O_3$ at 8.5 K. In the figure, positions (resonance fields) calculated for allowed and forbidden transitions are also shown (see text).
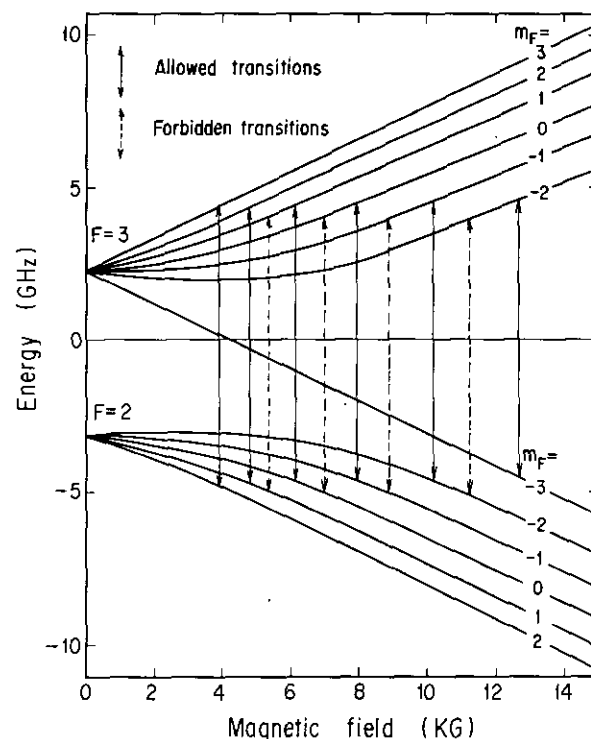
FIG. 2. Zeeman energy levels for Pr^{4+} in $BaCeO_3$. Arrows show the allowed and forbidden transitions.

+4.3 nuclear magnetons. The spin Hamiltonian for the EPR spectrum of $Pr^{4+}/BaCeO_3$ is

$$H = g\beta\mathbf{H}\cdot\mathbf{S'} + A\mathbf{I}\cdot\mathbf{S'} - g'_N\beta\mathbf{H}\cdot\mathbf{I}, \qquad [1]$$

where g is the g value for the Pr^{4+} with an effective spin $S' = \frac{1}{2}$, A is the hyperfine coupling constant, g'_N is the effective nuclear g value (in units of Bohr magnetons), β is the Bohr magneton, and $\mathbf{H}$ is the applied magnetic field. Usually the assumption can be made that the electronic Zeeman term (the first term on the right-hand side of Eq. [1] is much larger than the hyperfine term (second term on the right-hand side), which would result in a six-line spectrum for an isotropic resonance with $I = \frac{5}{2}$. In this case, this is a poor assumption and the above Hamiltonian must be solved exactly. The solution is well known (Breit–Rabi equation) and has been given by Ramsey (7) and others (8).

First, $\mathbf{I}$ and $\mathbf{S'}$ are coupled together to form the resultant $\mathbf{F}$, where $\mathbf{F} = \mathbf{I} + \mathbf{S'}$. For $S' = \frac{1}{2}$ and $I = \frac{5}{2}$ in the absence of a magnetic field, there are two states $F = 2$ and $F = 3$ which are separated by $3A$. When the magnetic field is included, each of these two states splits into $(2F + 1)$ $|m_F>$ Zeeman levels as shown in Fig. 2. Six allowed transitions ($\Delta F = \pm1$; $\Delta m_F = \pm1$) are observed along with five "forbidden" transitions ($\Delta F = \pm1$, $\Delta m_F = 0$, one of which overlaps with an allowed transition). The

assignments of these lines are shown in Fig. 1. With increasing temperature, all the assigned absorption lines become weaker in intensity and disappear above 160 K.

The absorption line centered at ca. 2940 G is not assigned to the Pr^{4+} ion. The temperature dependence of this EPR line is quite different from that of the others. Below 5.5 K, with decreasing temperature, this line saturates and becomes weaker and distorted in appearance. The assigned lines do not show this behavior. For this reason, we consider that this EPR line is not due to Pr^{4+}.

The results of fitting the observed EPR spectra to the parameters of the spin Hamiltonian (Eq. [1]) are shown in Table 1, with the best-fit parameters $|g| = 0.7451 \pm 0.0009$, $|A| = 0.0606 \pm 0.0002$, with g'_N set equal to 0.0. Because of the uncertainties in the measurements, it was not possible to obtain a meaningful value of g'_N. The measured hyperfine coupling constant is comparable to the value for Pr^{4+} in ZrSiO$_4$ ($A_\parallel = 0.06045$ cm^{-1}, $A_\perp = 0.0639$ cm^{-1}) (4).

Although the sign of the g value is not obtained by this measurement, comparison with other f^1 systems in octahedral symmetry, such as NpF$_6$/UF$_6$ (9) and Pa^{4+}/Cs$_2$ZrCl$_6$ (8), where the sign of the g value has been measured, indicates that the g value for Pr^{4+}/BaCeO$_3$ should be negative. The magnitude of the g value is very close to that of U^{5+} in NaUF$_6$ ($|g| = 0.746$) (10).

In the BaCeO$_3$ host material, the Pr^{4+} ion is substituted for the Ce^{4+} ion; i.e., it is in an octahedral site. For one f electron, the ^2F Russell–Saunders state breaks up into two J states, $J = \frac{5}{2}$ and $J = \frac{7}{2}$, when the effect of spin–orbit coupling is included. If we assume octahedral symmetry for the Pr^{4+} in BaCeO$_3$, the $J = \frac{5}{2}$ state breaks up into a doubly degenerate Γ_7 state and a fourfold degenerate Γ_8 state. The higher-lying $J = \frac{7}{2}$ state breaks up into two
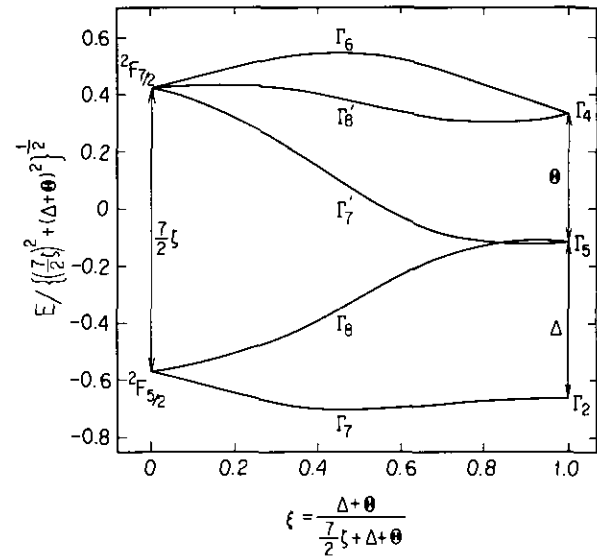

FIG. 3. Relative energy splittings of an f^1 electron as the relative magnitudes of the crystal field and spin–orbit coupling interactions change (octahedral symmetry).

doubly degenerate states, Γ_6 and Γ'_7, and a fourfold degenerate Γ'_8 state (see Fig. 3). The ground state in this symmetry is the $J = \frac{5}{2}$, Γ_7 state. The g value for the Γ_7 ground doublet in a pure $J = \frac{5}{2}$ manifold would be $-\frac{5}{3}$ times the Landé g factor. Since the Landé factor for the f^1 configuration is equal to $\frac{6}{7}$, the g value is $-\frac{10}{7}$. Indeed, the g value for Pa^{4+} in Cs$_2$ZrCl$_6$ is -1.142 (8). However, the crystal field interaction is not small as the spin–orbit coupling interaction, so the excited $J = \frac{7}{2}$, Γ'_7 state is mixed into the ground $J = \frac{5}{2}$, Γ_7 state via this interaction. The resulting expression for the ground state g value is given by

$$g = -2(\tfrac{5}{7}\cos^2\alpha - \tfrac{8}{21}\sqrt{3}\cos\alpha\sin\alpha - \tfrac{12}{7}\sin^2\alpha) \quad [2]$$

with

$$|\Gamma_7\rangle = \cos\alpha\,|J = \tfrac{5}{2}, \Gamma_7\rangle + \sin\alpha\,|J = \tfrac{7}{2}, \Gamma'_7\rangle. \quad [3]$$

With increasing admixture, the g value becomes larger, but can never exceed two. From the measured g value, the admixture of $J = \frac{7}{2}$, Γ'_7 state into the ground $J = \frac{5}{2}$, Γ_7 state is 2.6%.

To further analyze the electronic structure of Pr^{4+} in BaCeO$_3$ the energies of the crystal field levels must be known. To date the only measurement reported is the energy difference between the ground Γ_7 level and the first excited state, Γ_8, by inelastic neutron scattering in BaPrO$_3$ (5). For purposes of setting limits on the energy level splittings, we assume the spin–orbit coupling constant of Pr^{4+} is the same as that in the free ion, $\zeta_f = 865$ cm^{-1} (11). This assumption is an upper limit because in

$$\xi = \frac{\Delta + \theta}{\frac{7}{2}\zeta + \Delta + \theta}$$

TABLE 1
Experimental and Calculated Line Positions^a

Experimental		Calculated^b		
Allowed	Forbidden	Allowed	Fobidden	Difference exp − calc
12,652		12,665		−13
	11,206		11,160	46
10,147		10,201		−54
	8,870		8,851	19
7,918		7,927		−9
	6,930		6,927	3
6,137		6,132		5
	5,378		5,362	16
4,811		4,810		1
	—		3,886	—
3,873		3,886		−13

^{a} All values are given in gauss.

^{b} Spin-Hamiltonian parameters $|g| = 0.745 \pm 0.0009$, $|A| = 0.0606 \pm 0.0002$ cm^{-1}, g'_N set equal to 0.0.

f-element compounds, the spin–orbit coupling constant is usually reduced below the free-ion value.

The calculation of the energy levels of an f^1 configuration in an octahedral crystal field (O_h symmetry) is well known. It is convenient to use as the basis set the energy levels of the f^1 ion in a strong crystal field. Then the sevenfold orbitally degenerate f^1 ion is split into a singlet, Γ_2, and two triplets, Γ_4 and Γ_5. The Γ_2 level is lowest in energy and is set equal to zero. The energy differences between Γ_2 and Γ_5 is labeled Δ, and the energy difference between Γ_4 and Γ_5 is labeled Θ. This energy-level diagram is shown on the right-hand side of Fig. 3.

When spin–orbit coupling is taken into account, (with ζ the spin–orbit coupling constant), the Γ_2 orbital state is transformed into a doublet Γ_7, and the Γ_5 and Γ_4 states are split into Γ_7' (doublet) and Γ_8 (quartet) and Γ_6 (doublet) and Γ_8' (quartet), respectively. The ordering of the levels is shown in Fig. 3. The energy matrices for the Γ_7, Γ_8, and Γ_6 states are

$$\Gamma_7: \begin{vmatrix} 0 & \sqrt{3}\zeta \\ \sqrt{3}\zeta & \Delta - \frac{1}{2}\zeta \end{vmatrix}$$

$$\Gamma_8: \begin{vmatrix} \Delta + \frac{1}{4}\zeta & \frac{3}{4}\sqrt{5}\zeta \\ \frac{3}{4}\sqrt{5}\zeta & \Delta + \Theta - \frac{3}{2}\zeta \end{vmatrix} \qquad [4]$$

$$\Gamma_6: |\Delta + \Theta + \tfrac{3}{2}\zeta|.$$

Diagonalization of the Γ_7 energy matrix gives the ground state Γ_7 and the excited state Γ_7', and the corresponding wavefunctions are written as

$$|\Gamma_7\rangle = \cos\theta|^2F_{5/2}, \Gamma_7\rangle - \sin\theta|^2F_{7/2}, \Gamma_7'\rangle, \qquad [5]$$

where θ is the parameter describing the admixture of the Γ_7 levels in the ground state with the relation

$$\tan 2\theta = \frac{2\sqrt{3}\zeta}{\Delta - \frac{1}{2}\zeta}. \qquad [6]$$

The parameter θ in Eqs. [5] and [6] is related to the parameter α in Eq. [3] (12). The g value for the ground state Γ_7 doublet in the strong field basis set is

$$g = 2\langle\Gamma_7|L + 2S|\Gamma_7\rangle$$

$$= 2\cos^2\theta - \frac{4}{\sqrt{3}}\sin 2\theta. \qquad [7]$$

Using the Γ_7–Γ_8 splitting from Kern et al. (5) and the $Pr^{4+}/BaCeO_3$ g value given in this work and setting the spin–orbit coupling constant for Pr^{4+} at its free ion value of 865 cm^{-1}, we can determine the Θ and Δ values and calculate the energy levels. These data are collected in

TABLE 2
Energy Levels[a] and Parameters[b]
for $Pr^{4+}/BaCeO_3$

Γ_6	6501
Γ_8'	5398
Γ_7'	3248
Γ_8	2057[c]
Γ_7	0

[a] All values are given in cm^{-1}.
[b] $\zeta = 865$ cm^{-1}, $\Delta = 1686$ cm^{-1}, $\Theta = 2521$ cm^{-1}, g_{Γ_7}(calc) $= -0.743$.
[c] From Ref. (5).

Table 2. We can compare the parameter values with a number of $5f$ compounds of similar symmetry (13, 14) as shown in Table 3. Note that the crystal field splittings of $Pr^{4+}/BaCeO_3$ are much smaller than those for the actinide oxides. However we can use the measured g value vs the ratio of $\Delta/(\frac{3}{2}\zeta)$ as a measure of the relative strength of the crystal field to the spin–orbit splitting as shown in Fig. 4. By this measure $Pr^{4+}/BaCeO_3$ shows an appreciable crystal field strength relative to the spin–orbit splitting and is comparable to that of U^{5+} in UF_6^-. This ratio $\Delta/(\frac{3}{2}\zeta)$ in $Pr^{4+}/BaCeO_3$ is much greater than that found in the U^{5+} hexachloro- and hexabromo salts and for Ce^{3+} in $CeCl_6^{3-}$.

Since we have obtained the wavefunctions and energies for the ground and excited states, the magnetic susceptibility of $BaPrO_3$ is easily calculated with this model. The magnetic susceptibility for $BaPrO_3$ has been measured by three research groups (3, 15, 16), and the results are quite similar. This compound shows an antiferromagnetic transition at 11.5 K, which is supported by the λ-type specific heat anomaly at the same temperature (16). In the paramagnetic temperature region, the susceptibility follows the equation $\chi = 0.058/(T + 10.3) + 6.8 \times 10^{-4}$ emu/mole (3). Bickel et al. also obtained a quite similar susceptibility (15). From the temperature-dependent part of the susceptibility, the effective magnetic moment is calculated to be 0.68 μ_B. Our previous estimate for the g value from EPR was 0.86, from which the effective magnetic

TABLE 3
Spin-Orbit Coupling Constant and Crystal
Field Parameters[a]

Compound	ζ	Δ	Θ
$BaPrO_3$	865	1686	2521
$LiUO_3$	1938	3543	6145
Li_7UO_6	1868	4604	6600
Ba_3NpO_6	2378	5695	8800
Li_5PuO_6	2520	6700	5600

[a] All values are given in cm^{-1}.
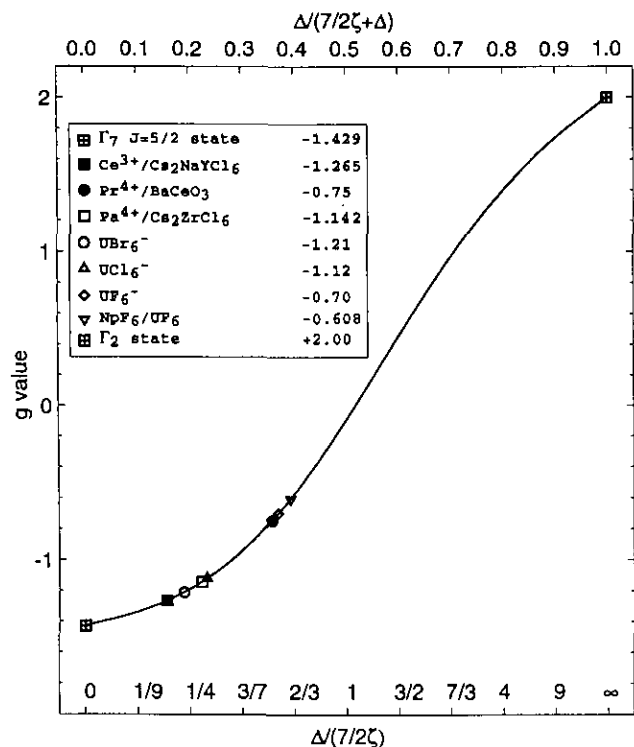
FIG. 4. g value vs the ratio $\Delta/(\frac{7}{2}\zeta)$ for a number of f^1 compounds in octahedral symmetry.

moment was calculated to be 0.74 μ_B from the relation $\mu_{\text{eff}} = g\sqrt{S'(S' + 1)}$. In that work, the g value was calculated from the average resonance field of the absorption lines split by the hyperfine interaction. In the present study, we have measured and analyzed the EPR spectrum of Pr^{4+} in BaCeO$_3$ and determined the g value to be 0.745, from which the effective magnetic moment is calculated to be 0.645 μ_B. This moment is quite close to the moment of BaPrO$_3$ (0.68 μ_B) derived from the magnetic susceptibility.

Next, the large temperature-independent paramagnetism is considered. Since this value is given by the equation (17)

$$\chi_{\text{TIP}} = 2N\beta^2 \sum_i \frac{|\langle\Gamma_i|L + 2S|\Gamma_7\rangle|^2}{E(\Gamma_i) - E(\Gamma_7)} \quad [8]$$

it is calculated to be 5.53×10^{-4} emu/mole, which is near the value from experiment, 6.8×10^{-4} emu/mole. Including Selwood's diamagnetic correction for BaPrO$_3$ (-62.83×10^{-6} emu/mole) gives much better agreement between experiment and calculation.

SUMMARY

The EPR spectrum of Pr^{4+} in BaCeO$_3$ has been analyzed. Based on this spectrum and data available from previous work, the optical spectrum of this system has been calculated. The measured magnetic susceptibility of the compound BaPrO$_3$ has been shown to be in reasonable agreement with the magnetic data obtained for Pr^{4+}/BaCeO$_3$ from the EPR experiment.

REFERENCES

1. T. Ringwood, *Am. Sci.* **70**, 201 (1982).
2. N. E. Topp, "Chemistry of the Rare-Earth Elements." Elsevier, Amsterdam, 1965.
3. Y. Hinatsu, *J. Solid State Chem.* **102**, 362 (1993).
4. E. Harris, J. H. Mellor, and S. Parke, *Phys. Status Solidi B* **122**, 757 (1984).
5. S. Kern, C.-K. Loong, and G. H. Lander, *Phys. Rev. B* **32**, 3051 (1985).
6. A. Abragam and B. Bleaney, "Electron Paramagnetic Resonance of Transition Ions," Chap. 5. Oxford Univ. Press, London, 1970.
7. N. F. Ramsey, "Molecular Beams." Clarendon Press, Oxford, 1956.
8. J. D. Axe, H. J. Stapleton, and C. D. Jeffries, *Phys. Rev.* **121**, 1630 (1961).
9. C. A. Hutchison and B. Weinstock, *J. Phys. Chem.* **32**, 56 (1960).
10. P. Rigny and P. Plurien, *J. Phys. Chem. Solids* **28**, 2589 (1967).
11. W. C. Martin, R. Zalubas, and L. Hagan, "Atomic Energy Levels—The Rare Earth Elements," NSRDS-NBS 60. U.S. Government Printing Office, Washington, DC, 1978.
12. A. Abragam and B. Bleaney, "Electron Paramagnetic Resonance of Transition Ions," Chap. 5, p. 358. Oxford Univ. Press, London, 1970.
13. Y. Hinatsu and N. Edelstein, *J. Solid State Chem.* **93**, 173 (1991).
14. Y. Hinatsu, T. Fujino, and N. Edelstein, *J. Solid State Chem.* **99**, 182 (1992).
15. M. Bickel, G. L. Goodman, L. Soderholm, and B. Kanellakopulos, *J. Solid State Chem.* **76**, 178 (1988).
16. J. B. Bulman, M. V. Kuric, R. P. Guertin, S. Foner, E. J. McNiff, Jr., G. Cao, J. O'Riely, J. E. Crow, P. P. Wise, and T. Yuen, *J. Appl. Phys.* **69**, 4874 (1991).
17. J. H. Van Vleck, "The Theory of Electronic and Magnetic Susceptibilities." Oxford Univ. Press, London, 1932.